



## Pair potential for Fe–He

N. Juslin\*, K. Nordlund

Department of Physics, University of Helsinki, P.O. Box 43, FI-00014, Helsinki 00014, Finland

### ARTICLE INFO

PACS:  
61.72.Ji  
61.43.Bn  
34.20.Cf

### ABSTRACT

A new potential for helium in bulk iron was developed in order to study the effect of He in irradiated iron. As helium in iron degrades the material properties, a good description of He defects is of importance for studying radiation damage with He present in iron. We show that a purely repulsive pair potential is enough to reproduce electronic structure calculations results from the literature for He defect formation and migration. *Ab initio* data for short range Fe–He dimer interaction is used to describe the high energy part of the potential.

© 2008 Elsevier B.V. All rights reserved.

### 1. Introduction

Helium present in iron, and in metals and materials in general, affects and usually deteriorates the structural and mechanical properties. He in iron is known to affect vacancy mobility and cause bubble formation, void swelling, high temperature embrittlement and blistering [1–6]. The steel in fusion reactors will be subject to 14 MeV neutron irradiation, which produces helium through (n, $\alpha$ ) transmutation reactions [7].

Many important processes of radiation damage are not easily available for experimental study, but are on time and length scales well suited for molecular dynamics (MD) and Monte Carlo studies. For example collision cascades have been extensively studied with MD simulations to determine primary damage formation in iron and iron-chromium [8,9], especially focusing on recent potentials developed with ferritic steels for reactors in mind [10]. The presence of helium, however, could affect the results by binding strongly to vacancies or helium-vacancy clustering, thus possibly affecting the recombination of damage.

Helium bubble formation and helium-vacancy clustering in iron has been studied [11–14] using a Fe–He pair potential by Wilson [15], which was not fitted to properties of helium in an iron matrix and is known to produce He defect energies in poor agreement with *ab initio* data [14]. The potential by Wilson gives the wrong order of stability for tetrahedral versus octahedral interstitials and a large difference compared to the stability of a substitutional He, as shown in Table 1. Recently an EAM type Fe–He potential was developed by Seletskaja et al. [16], which was fitted to helium defects in bulk iron.

While a pair potential should be enough to describe He in a material, since it is a noble gas element, Seletskaja et al. argue that

due to the magnetic properties of iron, many-body terms are needed to obtain the correct order of stability for helium in tetrahedral, octahedral and substitutional places [17,16]. The potential presented by Seletskaja et al. was, however, fitted with the Finnis–Sinclair iron potential [18] describing the Fe–Fe interaction. Our aim is to focus on more recent iron potentials to study radiation damage in iron and iron-chromium in the presence of He and need Fe–He, and in the future Cr–He, potentials better suited for them.

Here we present a Fe–He pair potential, using the Ackland–Mendelev potential [19] for the Fe–Fe interactions, which shows that a pair potential is enough to describe simple He defects and migration of He in iron. As a pair potential is computationally faster, as well as easier to implement in MD codes, than a many-body potential, it is advisable to use a pair potential when it is sufficient.

### 2. Data on He in Fe

For the high-energy interactions we calculated the total energy of the Fe–He dimer using density-functional theory (DFT) with the DMol97 program package [20,21]. To obtain the repulsive potential, the total energy was calculated as a function of the interatomic distance  $r$  at dense intervals. The standard DMol orbitals were augmented with hydrogenic orbitals [22]. This approach has previously been shown to give interaction energies in the repulsive region which agree well with a fully numerical Hartree–Fock–Slater ( $X_\alpha$ ) method [23,24].

This will be used at the short distances, which are important at high energies and do not matter for formation energies for He defects in the metal matrix. The dimer potential is, however, not adequate for describing helium defects in metals. The DMol data is presented in Fig. 1 and the numerical data needed to reproduce the potentials is listed in Table 3.

\* Corresponding author. Tel.: +358 919150079; fax: +358 919150042.  
E-mail address: [niklas.juslin@helsinki.fi](mailto:niklas.juslin@helsinki.fi) (N. Juslin).

**Table 1**  
Formation energies of helium interstitials in iron for substitutional, octahedral and tetrahedral positions

		Fe–Fe	Substitutional	Octahedral	Tetrahedral
DFT	Seletskaiia [17,16]	–	4.08	4.60	4.37
	Fu and Willaime [14]	–	4.22	4.57	4.39
MD	Wilson [14]	FS	3.25	5.25	5.34
	Seletskaiia [16]	FS	3.91	4.54	4.50
	This work:	AMS	4.10	4.51	4.39
		DUD	4.21	4.44	4.33
	FS	4.12	4.41	4.29	

All values are in eV. The Fe–Fe interactions are: FS = Finnis–Sinclair, AMS = Ackland–Mendelev, DUD = Dudarev–Derlet.

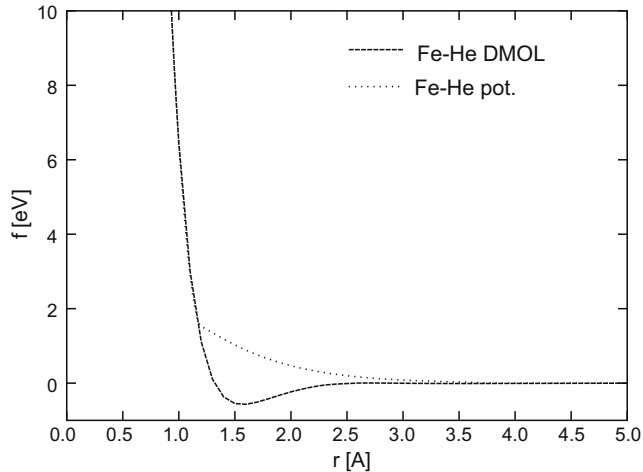


**Fig. 1.** The dimer potential from DMol DFT calculations and the Fe–He pair potential for describing He in an iron matrix. Clearly it is hard to construct a potential able to describe well both Fe–He molecules and He in bulk iron.

For helium defects in iron, DFT calculations have been made by Seletskaiia et al. [17,16] using the VASP code and Fu and Willaime [14] using the SIESTA code. As can be seen in Table 1, the Fe–He DFT results by different groups and methods do not agree completely, but the qualitative features are the same.

### 3. Potential construction

Finding a physically motivated function form that describes the energy and forces as a function of inter-atomic distance for the desired situations can be hard, due to limitations in MD, mainly since it treats atoms as spheres with no electrons and a limited interaction range. It would also be possible to use a numerical table and interpolate between points for a completely empirical potential, but this approach requires more DFT data to be reliable.

Considering the repulsive nature of helium in iron and the simplified picture of positive nuclei in an electron cloud, a natural function form to choose is a screened Coulomb potential. The function form  $f(r) = (a + b/r) \exp(-cr)$  was found to work well. Here the  $a$  and  $b/r$  terms give the ability to affect close and long range parts of the potential differently. Adding more terms and parameters would give more fitting options, but with limited data sets to fit to, would not guarantee a more transferable potential. It can be noted that already a simple  $a \exp(-cr)$  term is enough to give reasonable defect formation energies in the correct order.

The available *ab initio* data on interstitials does not provide any information for distances much shorter than the interatomic distances, and we can use either the data from the DMol calculations or the ZBL universal potential [25]. They are quite similar, but since we have the DFT data, we choose to use it. This choice does not affect the potential part fitted for larger distances. To get a smooth

transition between the two parts of the potential, we introduce a polynomial function fit to the values and derivatives at the transition points. In simulations close to equilibrium (kinetic energies less than about 2 eV) the atoms will not come close enough for the DMol part to be important and it is sufficient to use the function form. The potential form chosen is given by:

$$f(r_{ij}) = \begin{cases} \text{DMOL-potential}, & r_{ij} \leq r_1 \\ p_3 r_{ij}^3 + p_2 r_{ij}^2 + p_1 r_{ij} + p_0, & r_1 \leq r_{ij} \leq r_2, \\ \left(a + \frac{b}{r_{ij}}\right) e^{-cr_{ij}} f_c(r_{ij}), & r_{ij} \geq r_2, \end{cases} \quad (1)$$

where the cut-off function  $f_c$  is included for computational efficiency. It is given by:

$$f_c(r_{ij}) = \begin{cases} 1, & r_{ij} \leq r_c - r_d, \\ \frac{1}{2} \left(1 - \sin \frac{\pi(r_{ij} - r_c)}{2r_d}\right), & |r_c - r_{ij}| \leq r_d, \\ 0, & r_{ij} \geq r_c + r_d, \end{cases} \quad (2)$$

which is a function that goes smoothly from full interaction at  $r_{ij} \leq r_c - r_d$  to zero interaction at  $r_{ij} \geq r_c + r_d$ . This cut-off function is a standard type used e.g., in Tersoff type potentials [26].

The transition point and the cut-off parameters can partially be deduced based on the atom configurations around the helium atom for the defect structures of interest by considering the number of neighbors and their distances. It is, however, not always obvious where to cut off the potential and it affects the formation energies of the defects and migration energies, so trying different cut-offs is important.

For the fitting procedure we have compared the relaxed MD results with the relaxed DFT results. Trying to reproduce the exact DFT atom positions with our Fe–He potential would have been inadvisable, as the MD and DFT Fe–Fe interactions are not exactly the same. Thus, fitting to the DFT atom configurations would mean the Fe–He interaction compensates for differences in the iron part for these structures, which is not a desired property for a transferable potential. With good iron potentials, these differences can be expected to be quite small.

The function parameters were found by applying both a numerical fitting routine and manual fitting. The fitting routine was written to fit any given function to any defect atomic structure, where the defect atomic structure and Fe–Fe interaction energy were given by MD simulations with trial parameters and subsequently changed to new structures and energies. It can be noted that this step could have been done in the fitting routine by calculating the EAM interaction energies and forces for the iron atoms, and was done separately only due to programming reasons.

While the fitting routine gave acceptable results, we managed to further improve the potential by manually adjusting the parameters, since it is a rather complex process to decide what properties are desired and a human touch is often needed for finding the best parameters. The parameters are presented in Table 2.

All simulations were performed for 2000 atoms in pure bulk, adding and removing atoms as needed for the defects. The same

**Table 2**  
Parameters for the Fe–He potential

$a$ (eV)	26.65	$r_1$ (Å)	1.0	$p_3$ (eV/Å <sup>3</sup> )	62.020897
$b$ (eVÅ)	−15.0	$r_2$ (Å)	1.2	$p_2$ (eV/Å <sup>2</sup> )	−96.287579
$c$ (1/Å)	1.856	$r_c$ (Å)	3.7	$p_1$ (eV/Å)	−38.548739
		$r_d$ (Å)	0.25	$p_0$ (eV)	79.266283

results were obtained with 1024 atoms, indicating that the system was large enough. Periodic boundaries were used. The system was relaxed to 0 K and zero pressure, applying the Berendsen temperature and pressure control [27]. The potential was implemented in the MD code as a numerical table and the derivatives were calculated using cubic spline interpolation.

The Fe–Fe interaction clearly affects the neighborhood around the helium atom, and thus changing the potential for iron will affect the results. The change in the iron matrix due to a defect depends mainly on the stiffness of the potential. Since most potentials for an element are fit to similar elastic properties and defect properties, other potentials for Fe can be expected to produce He defect properties comparable to these, as can be seen in Table 1 for the Fe–He potential with three different Fe–Fe interactions. If intending to use another potential than the one by Mendev for iron [19], the properties should be tested and the Fe–He potential adjusted if necessary.

We emphasize that this potential is only suitable for helium in iron matrices and not for molecules. The DFT data in Fig. 1 would actually indicate a fairly strong binding, but it is well known that DFT methods tend to overestimate noble gas–metal interactions (in Ref. [14] comparison of DFT with more accurate quantum mechanical calculations showed this for FeHe). Moreover, no Fe–He molecules have yet been observed experimentally (the lightest noble gas for which a molecule has been reported is Ar [28]), so the lack of a Fe–He binding is not a significant problem in the present context.

#### 4. Results

The fitted properties are reproduced well, as can be seen in Table 1. We also show results for the Dudarev and Derlet [29]

**Table 3**  
Data listed for the Fe–He DMol dimer potential

$r$ (Å)	$f$ (eV)	$r$ (Å)	$f$ (eV)	$r$ (Å)	$f$ (eV)
0.001	742308.990941	0.100	3900.770613	0.560	83.527946
0.002	367929.108134	0.120	2932.205400	0.580	74.561277
0.003	243146.799839	0.140	2279.876865	0.600	66.673635
0.004	180789.363700	0.160	1814.874546	0.620	59.702486
0.005	143386.113350	0.180	1468.779606	0.640	53.513466
0.006	118462.568194	0.200	1202.690203	0.660	47.995909
0.007	100673.425256	0.220	993.428081	0.680	43.060309
0.008	87344.768144	0.240	826.385481	0.700	38.631227
0.009	76990.273923	0.260	691.670110	0.720	34.647305
0.010	68719.745430	0.280	582.160568	0.740	31.055904
0.011	61963.988467	0.300	492.614357	0.760	27.814882
0.012	56344.366351	0.320	418.974166	0.780	24.886748
0.013	51597.954831	0.340	358.075144	0.800	22.238914
0.014	47536.487083	0.360	307.477324	0.820	19.843742
0.015	44022.879513	0.380	265.243036	0.840	17.678637
0.016	40954.622254	0.400	229.812713	0.860	15.721379
0.017	38252.408019	0.420	199.952152	0.880	13.953087
0.018	35855.089452	0.440	174.682721	0.900	12.355634
0.019	33714.656575	0.460	153.202236	0.920	10.914554
0.020	31792.090048	0.480	134.857477	0.940	9.615746
0.040	13861.000825	0.500	119.113258	0.960	8.446703
0.060	8159.846377	0.520	105.536708	0.980	7.395154
0.080	5445.595238	0.540	93.772294	1.000	6.450862

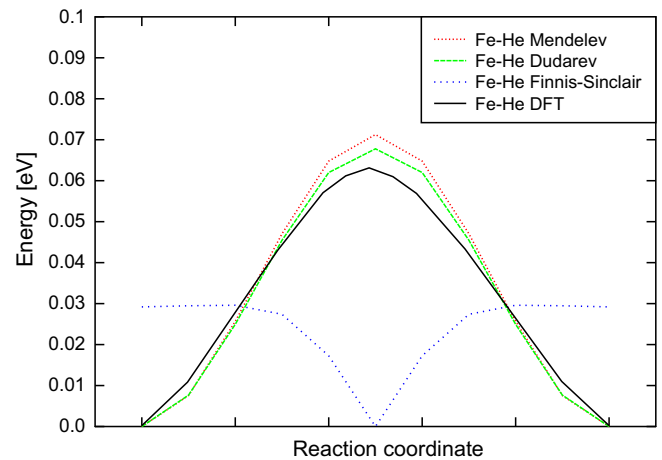


**Fig. 2.** The migration barrier for the migration of helium in iron from one tetrahedral interstitial position to a neighboring tetrahedral position. The results are in excellent agreement with the DFT data by Fu and Willaime [14]. Together with the Finnis–Sinclair Fe potential the He atom is slightly more stable midway between the two tetrahedral positions.

and the Finnis and Sinclair [18] iron potentials and note that the Fe–He potential produces acceptable results for these potentials as well. Comparing with the potential by Seletskaja et al., the formation energies of our potential are closer to DFT results.

We also compared the migration barriers of He defects with DFT results [14]. We calculated the migration of a tetrahedral interstitial He to a neighboring tetrahedral position using the drag method. We locked the He atom into place on the line between these positions and let the metal atoms around relax. We note that there are also other methods to calculate migration barriers, such as the nudged elastic band method [30], but the drag method was used in the DFT calculations and thus is best to use for this comparison. The results agree very well, as can be seen in Fig. 2. Using the Fe–Fe potential by Dudarev and Derlet also works well, but for the Finnis–Sinclair potential there is an energetically slightly more favorable place in the middle between the tetrahedral positions. The correct groundstate could be obtained by fitting for the Finnis–Sinclair potential.

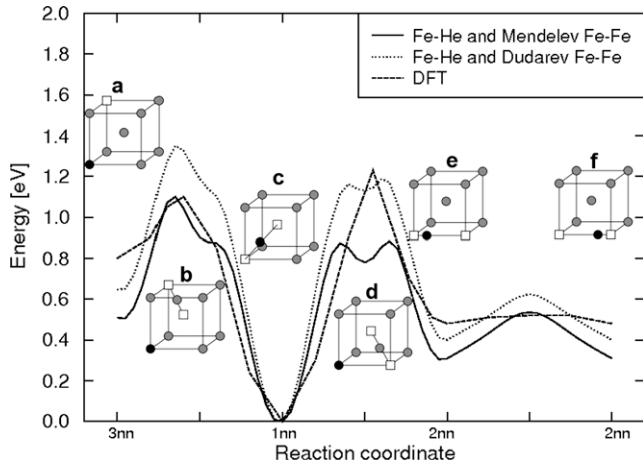


Fig. 3. The energy landscape for  $\text{HeV}_2$  in iron. As discussed in the text, the barriers are reasonable compared to DFT results by Fu and Willaime [14].

The migration of a substitutional He is more complicated and we need to consider the  $\text{HeV}_2$  complex as described by Fu and Willaime [14]. The energy landscape for this is shown in Fig. 3. We note generally good agreement, and the differences are mostly relatively small compared to the height of the barriers. The barrier between the second neighbor positions (e) and (f) is too high in the MD simulations. It was possible to make a potential with a lower barrier here, but not without losing the good defect properties. The double peak in case (d) is surprising. This is probably due to the cut-off function, but since we only have one data point from DFT in this region the mid point could be meta-stable in DFT as well. In either case, the relative depth of the well is so small that it does not matter much for migration from (c) to (d).

## 5. Conclusions

We have constructed the first available Fe–He potential for the Mendeleev iron potential and shown that a pair potential is enough to describe simple defect structures for helium in iron. The MD results agree well with the available DFT data, both for the formation and migration of defects. Providing an alternative to the old Wilson pair potential and the EAM type potential by Seletskaiia fitted using the Finnis–Sinclair iron potential gives a good opportunity to study whether differences in, e.g., helium–vacancy clustering emerge. Together with existing potentials and a Cr–He potential under development all needed interactions are soon available to simulate the effect of helium on damage production in iron–chromium alloys, as well as the pure elements.

## Acknowledgement

This work, supported by the European Communities under the contract of Association between EURATOM/Tekes, was carried out within the framework of the European Fusion Development Agreement. The views and opinions expressed herein do not necessarily reflect those of the European Commission. The research was performed within the Finnish Centre of Excellence in Computational Molecular Science (CMS), financed by The Academy of Finland and the University of Helsinki.

## References

- [1] S.E. Donnelly, J.H. Evans (Eds.), *Fundamental Aspects of Inert Gases in Solids*, Plenum, New York, 1991.
- [2] T. Ishizaki, Q. Xu, T. Yoshiie, S. Nagata, T. Troev, *J. Nucl. Mater.* 307–311 (2002) 961.
- [3] H. Trinkaus, B.N. Singh, *J. Nucl. Mater.* 323 (2003) 229.
- [4] M.B. Lewis, K. Farrell, *Nucl. Instrum. and Meth. B* 16 (1986) 163.
- [5] R. Vassen, H. Trinkaus, P. Jung, *Phys. Rev. B* 44 (1991) 4206.
- [6] B. van der Schaaf, D. Gelles, S. Jitsukawa, A. Kimura, R.L. Klueh, A. Mslang, G.R. Odette, *J. Nucl. Mater.* 283–287 (2000) 52.
- [7] R.E. Stoller, *J. Nucl. Mater.* 174 (1990) 289.
- [8] D. Terentyev, L. Malerba, R. Chakarova, C. Domain, K. Nordlund, P. Olsson, M. Rieth, J. Wallenius, *J. Nucl. Mater.* 349 (2006) 119.
- [9] C. Björkas, K. Nordlund, *Nucl. Instr. Meth. Phys. Res. B* 259 (2007) 853.
- [10] P. Olsson, J. Wallenius, C. Domain, K. Nordlund, L. Malerba, *Phys. Rev. B* 72 (2005) 214119.
- [11] K. Morishita, R. Sugano, B.D. Wirth, *J. Nucl. Mater.* 323 (2003) 243.
- [12] K. Morishita, R. Sugano, B.D. Wirth, T. Diaz de la Rubia, *Nucl. Instr. Meth. Phys. Res. B* 202 (2003) 76.
- [13] K. Morishita, R. Sugano, *J. Nucl. Mater.* 353 (2006) 52.
- [14] C. Fu, F. Willaime, *Phys. Rev. B* 72 (2005) 064117.
- [15] W.D. Wilson, in: *Conference on Fundamental Aspects of Radiation Damage in Metals*, USERDA-CONF-751006-P2, vol. 1025, 1975.
- [16] T. Seletskaiia, Y.N. Osetsk, R.E. Stoller, G.M. Stocks, *J. Nucl. Mater.* 351 (2006) 109.
- [17] T. Seletskaiia, Y. Osetsk, R.E. Stoller, G.M. Stocks, *Phys. Rev. Lett.* 94 (2005) 046403.
- [18] M.W. Finnis, J.E. Sinclair, *Philos. Mag. A* 50 (1984) 45.
- [19] G.J. Ackland, M.I. Mendeleev, D.J. Srolovitz, S. Han, A.V. Barashev, *J. Phys.-Condens. Mat.* 16 (27) (2004) S2629.
- [20] J. Delley, *J. Chem. Phys.* 92 (1990) 508.
- [21] DMol is a trademark of Accelrys, Inc.
- [22] Biosym Technologies Inc., San Diego, California, *DMol User Guide*, v. 2.3.5 Edition, 1993.
- [23] L. Laaksonen, P. Pyykkö, D. Sundholm, *Comput. Phys. Rep.* 4 (1986) 313.
- [24] K. Nordlund, N. Runeberg, D. Sundholm, *Nucl. Instr. Meth. Phys. Res. B* 132 (1997) 45.
- [25] J.F. Ziegler, J.P. Biersack, U. Littmark, *The Stopping and Range of Ions in Matter*, Pergamon, New York, 1985.
- [26] J. Tersoff, *Phys. Rev. Lett.* 56 (1986) 632.
- [27] H.J.C. Berendsen, J.P.M. Postma, W.F. Gunsteren, A.D. Nola, J.R. Haak, *J. Chem. Phys.* 81 (1984) 3684.
- [28] L. Khriachtchev, M. Pettersson, N. Runeberg, J. Lundell, M. Räsänen, *Nature* 406 (2000) 874.
- [29] S.L. Dudarev, P.M. Derlet, *J. Phys.-Condens. Mat.* 17 (2005) 1.
- [30] M. Villarba, H. Jonsson, *Surf. Sci.* 317 (1994) 15; G. Mills, H. Jonsson, G.K. Schenter, *Surf. Sci.* 324 (1995) 305.